JCTC Journal of Chemical Theory and Computation

Photoisomerization Reactions of Cyclopropene and 1,3,3-Trimethylcyclopropene: A Theoretical Study

Ming-Der Su*

Department of Applied Chemistry, National Chiayi University, Chiayi 60004, Taiwan

Received March 6, 2008

Abstract: The mechanisms of the photochemical isomerization reactions were investigated theoretically using two model systems, cyclopropene and 1,3,3-trimethylcyclopropene with the CASSCF/6−311G(d) (six-electron/six-orbital active space) and MP2-CAS/6−311G(d,p)//CASSCF/6−311G(d) methods. The structures of the conical intersections, which play a decisive role in such photorearrangements, were obtained. The intermediates and transition structures of the ground states were also calculated to assist in providing a qualitative explanation of the reaction pathways. Our model investigations suggest that the preferred reaction route for both cyclopropene and 1,3,3-trimethylcyclopropene is as follows: reactant → Franck−Condon region → local minimum → transition state → conical intersection → local intermediate → transition state → photoproduct. The theoretical findings suggest that the conical intersection mechanism found in this work gives a good explanation and supports the experimental observations. We also investigated the thermal (dark) reaction mechanisms for the hydrogen migration reactions. Again, all the relative yields of final products predicted based on the present work are in good agreement with the available experimental findings.

I. Introduction

Experimentalists and theoreticians alike have been long fascinated by the inclusion of double bonds in small carbocyclic rings.[1] For instance, the chemical and physical properties of the ground- and excited-state potential energy surfaces which link the cyclopropene (C_3H_4) hydrocarbons have been the subject of considerable experimental and theoretical investigations over many years.[2] Nevertheless, the photochemistry of cyclopropenic compounds has drawn surprisingly little attention.[3] The first report of cyclopropene photolysis appeared in the work of Chapman.[4] He reported that photolysis of cyclopropene itself (**1**) in an argon matrix at 8 K (eq 1 in Scheme 1) yields allene (**2**) and propyne (**3**). However, the relative yields of the two photoproducts have never been reported. On the other hand, thermolysis of cyclopropene at 190−240 °C yields **2** and **3** in yields of 1−2% and ca. 98%, respectively.[5]

Also, other intriguing photochemical results have been found in an unsymmetrical, alkyl-substituted cyclopropene (1,3,3-trimethylcyclopropene, **4**). See eq 2 in Scheme 1. This study represents the first investigation of the photochemistry of monocyclic, alkyl-substituted cyclopropene derivatives in solution. Photolysis of **4** in hydrocarbon solution with far-uv light results in rearrangement to the five primary products (**5**−**9**) shown in eq 2.[3,6] Similar product yields have been observed in the thermolysis of **4**. Gas-phase thermolysis of

Scheme 1

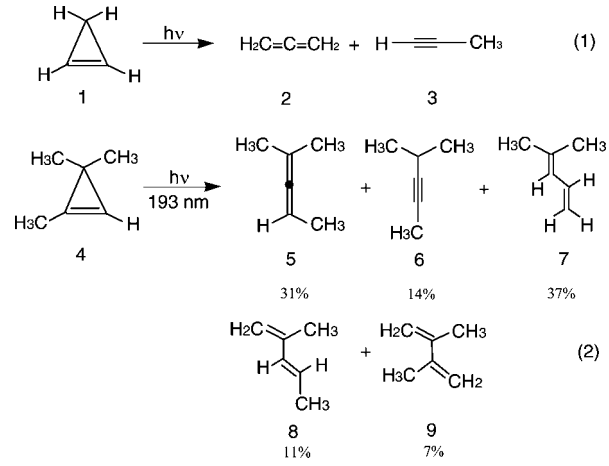

* Corresponding author e-mail: midesu@mail.ncyu.edu.tw.

10.1021/ct800078j CCC: $40.75
Published on Web 06/21/2008

4 has been reported to produce **8** and **9** in yields of 71 and 21%, respectively; no other products were reported.[7] Leigh and Fahie considered that most of the photolysis products are formally derived from the vinylcarbene formed by cleavage of the more highly substituted cyclopropene σ-bond in the excited singlet state. Moreover, two-bond cleavage of excited cyclopropenes to yield carbenes and alkynes is unimportant in solution, even for cyclopropenes with high excitation energies.[6] However, to the best of our knowledge, until now no theoretical investigations have been devoted to the study of such photochemical isomerization reactions.

Since the photochemical rearrangements of cyclopropene and its related compound mentioned above are both unusual and useful, we were curious about exactly how they occur and wanted detailed mechanistic knowledge in order to exercise greater control over them. Although these experimental results help in understanding the potential energy surfaces of excited states in cyclopropene systems, they are at present not capable of providing complete mechanistic detail. In fact, a detailed understanding of the photochemical reactions of cyclopropene as well as its derivatives is of interest not only for the advancement of basic science but also for further precise control of the total reaction process.

In principle, most photochemical reactions of organic molecules start on an excited electronic potential surface but cross over to a lower surface somewhere along the reaction pathway.[8,9] They finally reach the ground-state surface by a sequence of radiationless transitions (i.e., conical intersections) and move on the ground-state surface toward the product.[8] This mechanism is not controlled by the avoided surface crossing and the resulting energy gap between ground and excited states but rather by the presence of minima and transition states on the ground and excited states themselves. Furthermore, the existence of a conical intersection region provides access to a number of ground-state pathways that can lead to different photoproducts.[10] Indeed, interest in the area of photochemistry over the past decade has remained high as a result of a number of efforts focusing on excited-state processes that are promoted by conical intersections. This has already been both experimentally and theoretically proved to be a general feature of the excited states relevant to photochemical reactions.[11]

In order to understand the reaction mechanism of the photoreactions of cyclopropenes,[8–11] we have undertaken an investigation of the potential energy excited-state surfaces of C_3H_4 (**1**) and C_6H_{10} (**4**) in their singlet states. It is the aim of this paper to generate the essential parts of the potential surfaces by quantum chemical calculations and to describe the consequences for the reaction mechanisms from such an explicit calculation of the reaction pathways. It will be shown below that the conical intersection[10,11] plays a crucial role in the photochemistry of cyclopropenes systems.

II. Methology

All the geometries were fully optimized without imposing any symmetry constraints, although in some instances the resulting structures showed various elements of symmetry. The *ab initio* molecular orbital calculations were performed using the Gaussian 03 software package.[12]

In the investigation of the photochemical reaction pathways, the stationary point structures on the S_0 and S_1 surfaces were optimized at the CASSCF (the complete-active-space SCF) level of calculations using the standard 6−311G(d) basis set.[13] The active space for describing the photoisomerizations of **1** and **4** comprises six electrons in six orbitals, i.e., two p-π orbitals plus two σ(C−C) and two σ*(C−C) orbitals. This is referred to as CASSCF(6,6). In some hydrogen shift molecules, their active space is chosen as two p-π orbitals plus two σ (i.e., C−C and C−H) and two σ* (i.e., C−C and C−H) orbitals. The state-averaged CASSCF(6,6) method was used to determine geometry on the intersection space. The optimization of conical intersections was achieved in the (f - 2)-dimensional intersection space using the method of Bearpark et al.[14] implemented in the Gaussian 03 program.

Every stationary point was characterized by its harmonic frequencies computed analytically at the CASSCF level. The harmonic vibrational frequencies of all the stationary points were computed analytically to characterize them as minima (all frequencies are real) or transition states (only one imaginary frequency). The optimization was determined when the maximum force and its root-mean-square (rms) were less than 0.00045 and 0.00005 hartree/bohr, respectively. For each transition state, an IRC (CASSCF) calculation[15] has been performed as well. Accordingly, the products and reagents connected by the respective transition states have been unambiguously localized. The IRC results are given in the Supporting Information. Localization of the minima, transition states, conical intersection minima, and mapping of the intrinsic reaction coordinates has been performed in mass-weighted Cartesian coordinates; therefore, the results are independent of any specific choice of internal variables.

To correct the energetics for dynamic electron correlation, we have used the multireference Møller−Plesset algorithm[16] as implemented in the program package GAUSSIAN 03. Unless otherwise noted, the relative energies given in the text are those determined at the MP2-CAS-(6,6)/6−311G(d,p) level using the CAS(6,6)/6−311G(d) (hereafter designed MP2-CAS and CASSCF, respectively) geometry.

III. General Consideration

Even though the cyclopropene and cyclopropene derivative photoisomerization reported experimentally[3,6,7] show wide variance in their reaction types, it is possible to construct a certain consistency in these reactions, which at least serves as a basis for discussion. In this section, we describe possible excited-state reaction paths that lead to the conical intersections. It has been shown that thermolysis of cyclopropenes results in the formation of products consistent with initial ring opening to yield vinylcarbene intermediates.[3,17] Also, it has been found that the same situation occurs during the photolysis of cyclopropenes.[6,17] Basically, thermochemical cyclopropene ring opening produces the S_0 state (σ^2), whereas photochemical ring opening is considered to involve the S_1 state (σp; planar vinyl diradical).[3,17] See Scheme 2. Moreover, according to previous theoretical calculations, it was noted that the lowest excited triplet state of cyclopropene

Scheme 2

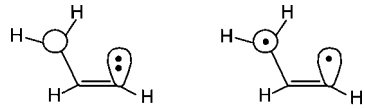

vinylmethylene

is unreactive toward ring opening and generally undergoes dimerization.[3,18] We thus do not consider the excited triplet state any further.

Again, in the case of eq 2, Leigh and Fahie proposed a mechanism involving the vinylcarbene intermediate to explain the formation of a variety of photoproducts due to the photolysis of **4**.[3,6] As demonstrated in Scheme 3, they concluded that 70−90% of the observable products are derived from the two possible vinylcarbene intermediates (**10** and **11**) formed from **4**.[3,6] Namely, they suggested that the photoproducts **5**−**8** should result from the vinylcarbene **10** formed by cleavage of the more highly substituted cyclopropene single bond in **4**, whereas only diene **9** derives from the vinylcarbene **11** obtained by cleavage of the less substituted cyclopropene single bond. Further supporting evidence comes from the fact that, according to the bond order analysis based on the CAS(6,6)/6−311G(d) level of theory, it was found that the C−C bond order increases in the order C_1-C_3 (1.042) < C_2-C_3 (1.082) < C_1-C_2 (1.175) at the S_1 excited state of 1,3,3-trimethylcyclopropene (**4**). Since it is well-known that absorption of light leads to cleavage of the weakest of the chemical bonds in the ring,c one may predict that bond cleavage should decrease in the order $C_1-C_3 > C_2-C_3 > C_1-C_2$. That is to say, the most substituted (C_1-C_3) 1,3,3-trimethylcyclopropene (**4**) single bond should be more easily broken than the less substituted (C_2-C_3) **4** single bond. From the above discussion, it is clear that vinylcarbene intermediates should play a central role in the photochemical mechanisms of cyclopropene and its derivatives. Nevertheless, attempts to chemically trap such intermediates using methanol or alkene have all been unsuccessful.[6]

We shall use the above ideas to help locate the "funnel" from the excited-state surface to the ground-state surface that corresponds to a conical intersection in the following section.

IV. Results and Discussion

(1) Cyclopropene (C_3H_4). Let us first consider the photoisomerizations of cyclopropene (**1**). For an understanding of its both ground- and excited-state mechanism, it is best to start the discussion with the reaction profiles as summarized in Figure 1, which also contains the relative energies of all the critical points with respect to the energy of the reactant **1**. Some selected geometrical parameters optimized for the stationary points and conical intersections are collected in Figure 2. The energies relative to the reactant molecule (**1**) are also listed in Table 1. Cartesian coordinates and energetics calculated for the various points at the CASSCF/6−311G(d) level are available as Supporting Information.

Our theoretical investigations are based on the mechanism indicated in Figure 1. In the first step the reactant (cyclopropene, **1**) is promoted to its excited singlet state by a vertical excitation as shown in the left-hand of Figure 1. After the vertical excitation process, the molecule is situated on the excited singlet surface but still possesses the S_0 (ground-state) geometry (**FC-1**).[15] The vertical excitation energy ($S_0 \rightarrow S_1(S_0$ geom)) was calculated to be 169 and 200 kcal/mol at the MP2-CAS and CASSCF levels of theory. As there are no relevant experimental and theoretical data on the cyclopropene system, the above result is a prediction.

From the point reached by the vertical excitation $S_1(S_0$ geom), the molecule relaxes to a local minimum **Int-1** ($S_1(S_1$ geom)),[19] which is predicted to be 60 kcal/mol lower in energy than **FC-1** ($S_1(S_0$ geom)). The optimized geometrical parameters of **Int-1** ($S_1(S_1$ geom)) are given in Figure 2. Comparing the **Int-1** geometry (Figure 2) with that of its corresponding ground-state minimum **1** (Figure 2), it is readily seen that the former has one significantly longer C−C bond (1.827 Å) and two somewhat shorter C−C bonds (1.472 and 1.449 Å) than its closed shell singlet state. As a result, the three-membered ring in the intermediate **Int-1** is to some extent broken. From this local minimum, **Int-1**, a transition state search for the ring-opening based on the model of the **Int-1** conformation was investigated. As can be seen in Figures 1 and 2, the cyclopropene ring opening process proceeds via a transition state **TS-1** (and **TS-1′**). Vibrational frequency calculations show that **TS-1** (and **TS-1′**) is a real transition state with one imaginary frequency (1047*i* and 927*i* cm^{-1}) on the singlet potential energy surface. Our MP2-CAS calculation predicts that this route possesses a small barrier, of about 12 kcal/mol. Due to the large excess energy of about 60 kcal/mol resulting from the relaxation from **FC-1** ($S_1(S_0$ geom)) to **Int-1** ($S_1(S_1$ geom)), the barrier can easily be surmounted.

From the **TS-1** point cyclopropene reaches an S_1/S_0 **CI** where the photoexcited system decays nonradiatively to S_0. Specifically, the photochemically active relaxation path, starting from the **TS-1** excited-state of cyclopropene, leads to either S_1/S_0 **CI-c-1** (path 1) or **CI-t-1** (path 2). As already mentioned in the previous section, one may foresee that the vinylcarbene-like species (**CI-c-1** and **CI-t-1**) should play a key role in the photorearrangement reactions of **1**. That is, along the C_1C_2 bending reaction path, two conical intersections, **CI-c-1** and **CI-t-1**, are obtained at the $\angle C_1C_2C_3$ bond angle of 123° and 125°, respectively. Their optimized structures are given in the left- and right-hand side of Figure 2 along with several key structural parameters. Moreover, the energy difference between these two conical intersections is only 1.1 kcal/mol, the former being lower than the latter, at the MP2-CAS level of theory. In Figure 2, we also give the directions of the derivative coupling and gradient difference vectors for both S_1/S_0 **CI-c-1** and **CI-t-1** conical intersections. As a result, for instance, funneling through the S_1/S_0 **CI-c-1** conical intersection leads to two different reaction pathways on the ground-state surface via either the derivative coupling vector or the gradient difference vector.[10] Any linear combination of these vectors causes the degeneracy to be lifted, and therefore these vectors give an

Scheme 3

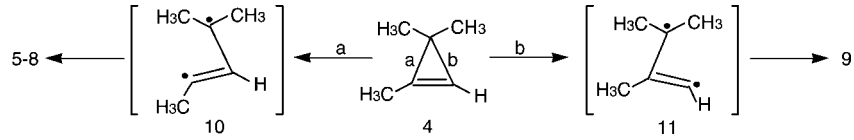

indication of possible reaction pathways available on the ground-state surface after decay. According to the results demonstrated in Figure 2, examination of these two vectors in **CI-c-1** provides important information about the photoisomerization process of **1**: the major contribution to the derivative coupling vector involves C−C bond stretching that gives the planar **Int-c-2** intermediate on the S_0 surface. However, the gradient difference vector gives an asymmetric CCC bending motion that leads to a vibrationally hot **1**-S_0 species. Similarly, this phenomenon can also be found in path 2. That is, as shown in Figure 2, the derivative coupling vector of **CI-t-1** results in the planar **Int-t-2** intermediate, while its gradient difference vector gives a vibrationally hot **1**-S_0 species.

From these local minima (**Int-c-2** and **Int-t-2**), a hydrogen migration must take place via transition states (**TS-c-2** and **TS-t-2**) to give the final products **2** and **3**, respectively. Our theoretical findings indicate that both hydrogen migration pathways possess their own barrier heights, computed to be

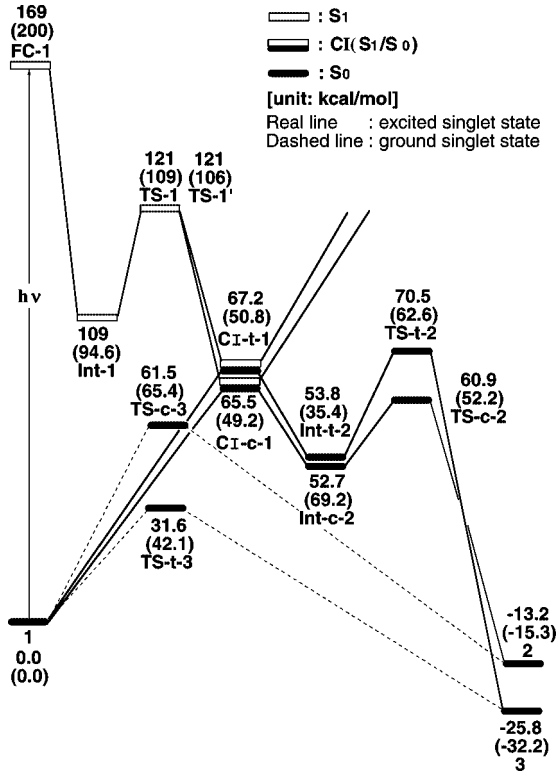

Figure 1. Energy profiles for the photoisomerization modes of cyclopropene (**1**). The abbreviations FC and CI stand for Frank-Condon and conical intersection, respectively. The relative energies were obtained at the MP2-CAS-(6,6)/6−311G(d,p)//CAS(6,6)/6−311G(d) and CAS(6,6)/6−311G(d) (in parentheses) levels of theory. All energies (in kcal/mol) are given with respect to the reactant (**1**). The CASSCF optimized structures of the crucial points, see Figures 2 and 3. For more information see the text.

17 kcal/mol for the formation of allene **2** (path 2) and 8.2 kcal/mol for the production of propyne **3** (path 1). Additionally, both photoproducts **2** and **3** are thermodynamically stable by 13 and 26 kcal/mol compared with reactant **1**, respectively. Thus, our computational results suggest that the mechanisms for path 1 and path 2 should proceed as follows:

$$\text{Path 1: } \mathbf{1}(S_0) + h\nu \rightarrow \mathbf{FC-1} \rightarrow \mathbf{Int-1} \rightarrow \mathbf{TS-1} \rightarrow \mathbf{CI-t-1} \rightarrow \mathbf{Int-t-2} \rightarrow \mathbf{TS-t-2} \rightarrow \mathbf{3} \quad (1)$$

$$\text{Path 2: } \mathbf{1}(S_0) + h\nu \rightarrow \mathbf{FC-1} \rightarrow \mathbf{Int-1} \rightarrow \mathbf{TS-1} \rightarrow \mathbf{CI-c-1} \rightarrow \mathbf{Int-c-2} \rightarrow \mathbf{TS-c-2} \rightarrow \mathbf{3} \quad (2)$$

Furthermore, from the computational data discussed above, one can readily see that the barrier to path 1 is larger than that for path 2, by 8.5 kcal/mol in energy. This finding suggests that path 2 should be more favorable than path 1 from a kinetic viewpoint. Based on the present theoretical investigations as demonstrated in Figure 1 and Table 1, we thus predict that the photoproduct (allene, **2**) produced by path 2 should be in a larger quantum yield than the photoproduct (propyne, **3**) produced by path 1 (see below).

On the other hand, we have also examined the dark (thermal) reaction on the ground-state potential energy surface. Although photoexcitation raises cyclopropene into an excited electronic state, the products of the photochemical process are controlled by the ground-state (thermal) potential surface.[7] Two reaction pathways (path 3 and path 4) were thus explored in this work. The search for transition states on the S_0 surface near the structures of **CI-c-1** and **CI-t-1** gives **TS-c-3** and **TS-t-3** for the products allene **2** (path 4) and propyne **3** (path 3), respectively. The optimized geometrical parameters of these transition states are collected in Figure 3. In addition, the MP2-CAS computational results indicate that the energy of **TS-c-3** relative to the ground-state minimum (**1**) is 62 kcal/mol and lower than the S_1/S_0 **CI-c-1** by only 4.0 kcal/mol. Nevertheless, the energy of the **TS-t-3** connecting **1** and **3** on the S_0 surface lies 32 kcal/mol above the energy of reactant **1**. This strongly suggests that in the dark reaction path 3 (formation of propyne **3**) is more favorable than path 4 (formation of allene **2**). Thus, our theoretical calculations demonstrate that both thermal reactions, path 3 and path 4, can be represented as follows:

$$\text{Path 3: } \mathbf{1} \rightarrow \mathbf{TS-t-3} \rightarrow \mathbf{3}$$

$$\text{Path 4: } \mathbf{1} \rightarrow \mathbf{TS-c-3} \rightarrow \mathbf{2}$$

Based on the above discussion, we can then propose a picture of the photochemistry of **1**, which is already shown schematically in Figure 1. Comparing the two reaction pathways (path 1 and path 2), our *ab initio* CASSCF and MP2-CAS calculations show that path 2 is preferred over path 1. That is, an efficient photoisomerization occurs when the photoexcited reactant **FC-1** evolves along a small barrier excited-state pathway, decays at a conical intersection point

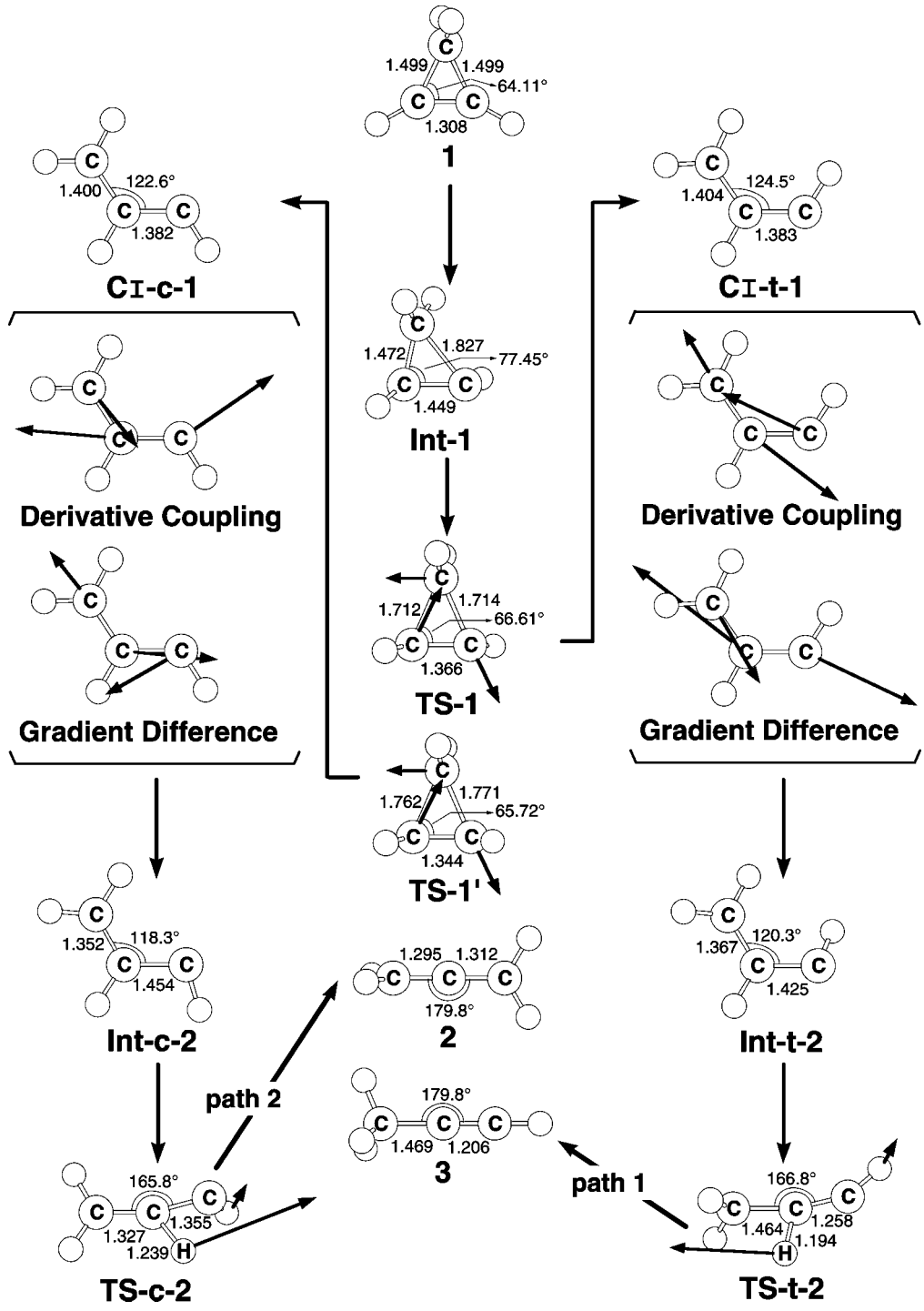

Figure 2. The CAS(6,6)/6−311G(d) geometries (in Å and deg) for path 1 and path 2 of cyclopropene (**1**), conical intersection (**CI**), intermediate (**Int**), transition state (**TS**), and isomer products. The derivative coupling and gradient difference vectors—those which lift the degeneracy—computed with CASSCF at the conical intersections **CI-c-1** and **CI-t-1**. The corresponding CASSCF vectors are shown inset. Also, the heavy arrows indicate the main atomic motions in the transition state eigenvector. For more information see the Supporting Information.

(S_1/S_0 **CI-c-1** or **CI-t-1**),[15] and finally relaxes to the ground-state between reactant (**1**) and photoproduct allene (**2**) or propyne (**3**), respectively. Also, our theoretical investigations strongly predict that the quantum yield of allene **2** should be greater than that of propyne **3** from a kinetic viewpoint. As mentioned earlier, neither experimental nor theoretical work on such a molecule has been reported so far.

However, in the dark (thermal) reaction the above situation is completely inverted. In the competition between the formation of allene **2** (path 4) and propyne **3** (path 3), the former has the larger energy requirement and the lower exothermicity. As a result, this makes path 3 the most energetically favorable pathway for thermal cyclopropene isomerization. In principle, these two reactions are concerted C−C bond cleavage accompanied by 1,2-H shift. Accordingly, one can foresee that in the dark reaction the yield of propyne **3** should be larger than that of allene **2.** This conclusion is in good agreement with experimental observations.[5]

Table 1. Energies (in kcal/mol) of the Critical Points Located along the Pathways 1-4 at the MP2-CAS(6,6)/6-311G(d,p)//CAS(6,6)/6-311G(d) and CAS(6,6)/6-311G(d) (in Parentheses) Levels of Theory[a]

structure	state	ΔErel[b]
cyclopropene **(1)**	S_0	0.0 (0.0)
FC-1	S_1	168.9 (199.6)
Int-1	S_1	108.6 (94.57)
TS-1	S_1	120.8 (109.2)
CI-t-1	S_1/S_0	67.23 (50.83)
TS-1′	S_1	120.5 (106.3)
CI-c-1	S_1/S_0	65.47 (49.20)
Int-t-2	S_0	53.78 (35.44)
Int-c-2	S_0	52.71 (69.23)
TS-t-2	S_0	70.46 (62.64)
TS-c-2	S_0	60.89 (52.20)
TS-t-3	S_0	31.61 (42,12)
TS-c-3	S_0	61.54 (65.42)
alene **(2)**	S_0	−13.15 (−15.32)
propyne **(3)**	S_0	−25.84 (−32.18)

[a] See Figures 2 and 3. [b] Energy relative to cyclopropene.

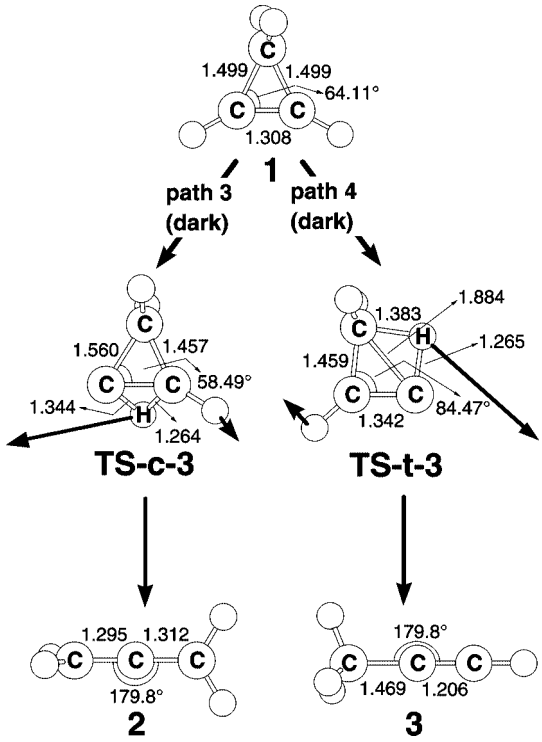

Figure 3. The CAS(6,6)/6−311G(d) geometries (in Å and deg) for path 3 and path 4 of cyclopropene (**1**), transition state (**TS**), and isomer products in the dark (thermal) reactions. The heavy arrows indicate the main atomic motions in the transition state eigenvector. For more information see the Supporting Information.

Furthermore, as already shown in Figures 1 and 2, our theoretical computations strongly demonstrate that both photolysis and thermolysis of cyclopropene (**1**) can be formally attributed to the initial formation of the vinylcarbene intermediate. This is consistent with what we predicted in the previous section.

(2) 1,3,3-Trimethylcyclopropene (C_6H_{10}). Next, we consider the photochemical rearrangement reactions of 1,3,3-trimethylcyclopropene (**4**). As stated earlier, there are two kinds of reaction pathways for the photoisomerization

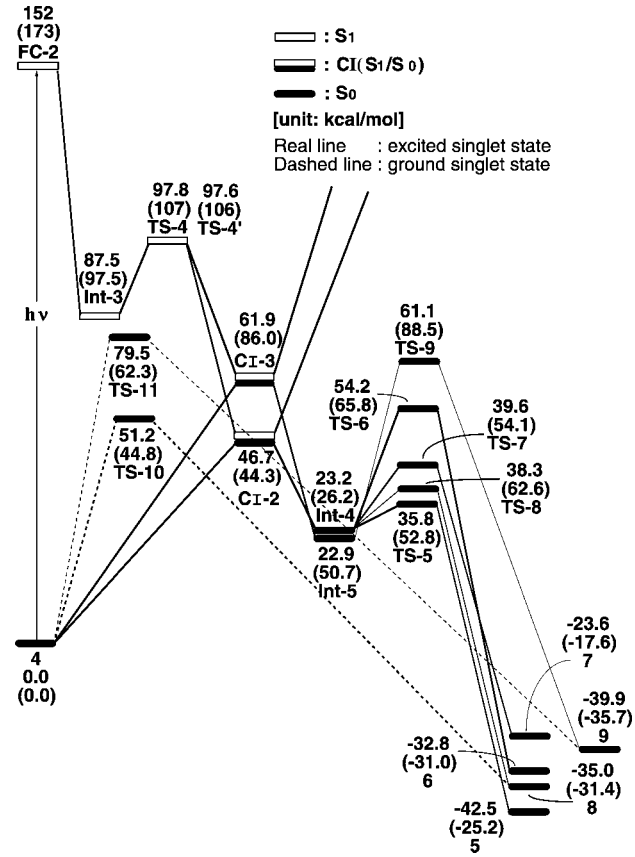

Figure 4. Energy profiles for the photoisomerization modes of 1,3,3-trimethylcyclopropene (**4**). The abbreviations **FC** and **CI** stand for Frank-Condon and conical intersection, respectively. The relative energies were obtained at the MP2-CAS(6,6)/6−311G(d,p)//CAS(6,6)/6−311G(d) and CAS(6,6)/6−311G(d) (in parentheses) levels of theory. All energies (in kcal/mol) are given with respect to the reactant (**4**). The CASSCF optimized structures of the crucial points, see Figures 5 and 6. For more information see the text.

reactions of **4**, i.e., path 5 and path 6, which may lead to the final photoproducts as given in Scheme 1. Figure 4 shows the reaction profiles computed for eq 2 and contains the relative energies of the various points with respect to the energy of the reactant **4**. Selected geometrical values and the relative energies based on the CASSCF and MP2-CAS calculations for all the stationary points of **4** are reported in Figures 5 and 6 and Table 2, respectively. Cartesian coordinates are given in the Supporting Information.

The vertical excitation energy (**FC-2**) is calculated to lie 173 kcal/mol above the ground-state surface at the CAS(6,6)/6−311G(d) optimized reactant geometry of **4**. This value drops to 152 kcal/mol after correction using MP2-CAS calculations, which is surprisingly close to the experimental absorption band (193 nm = 148 kcal/mol).[6] It is thus believed that the present model compound with the current method employed in this study should provide reliable information for the discussion of the singlet photochemical reaction mechanisms of **4**.

Once $S_0 \rightarrow S_1$ vertical excitation occurs, the system will relax from the **FC-2** point ($S_1(S_0$ geom)) to the S_1 minimum **Int-3** ($S_1(S_1$ geom)), the latter being lower in energy by 65 kcal/mol than the former. The optimized geometrical pa-

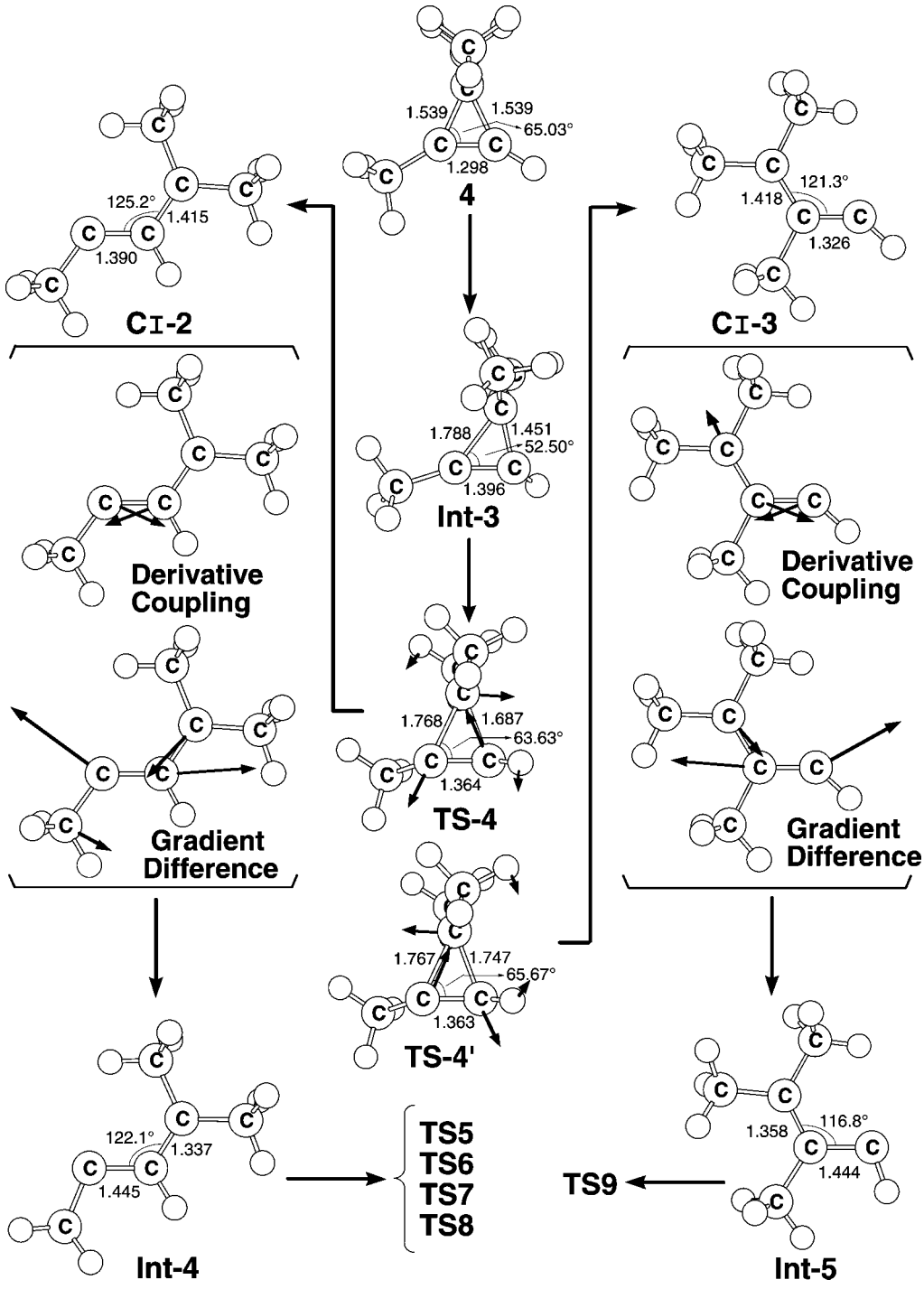

Figure 5. The CAS(6,6)/6−311G(d,p) geometries (in Å and deg) for path 5 and path 6 of 1,3,3-trimethylcyclopropene (**4**), conical intersection (**CI**), intermediate (**Int**), and transition state (**TS**). The derivative coupling and gradient difference vectors—those which lift the degeneracy— computed with CASSCF at the conical intersections **CI-3**. The corresponding CASSCF vectors are shown inset. Also, the heavy arrows indicate the main atomic motions in the transition state eigenvector. For more information see the Supporting Information.

rameters of **Int-3** can be found in Figure 5. As with the case of cyclopropene (**1**), our CASSCF results indicate that the **Int-3** structure has two short C−C bonds (1.420 and 1.428 Å) and one longer bond one (1.872 Å) compared with its closed shell singlet state. Again, this strongly implies that one C−C bond of the triangular ring (**Int-3**) is broken during the photochemical isomerization of **4**.

After the local minimum **Int-3**, we located two transition states **TS-4** and **TS-4′**, which are based on the model of reactant **4**. The optimized transition states structure (**TS-4** and **TS-4′**) along with the calculated transition vectors at the CASSCF level are given in Figure 5. The arrows indicate the direction in which the three carbon atoms in the 3-membered ring vibrate in the normal coordinate corresponding to the imaginary frequency (750*i* and 726*i* cm^{-1}). As seen in Figure 4 and Table 2, it is apparent that the transition structure (**TS-4**) for the ring opening process is lower in energy, by 54 kcal/mol, than the corresponding

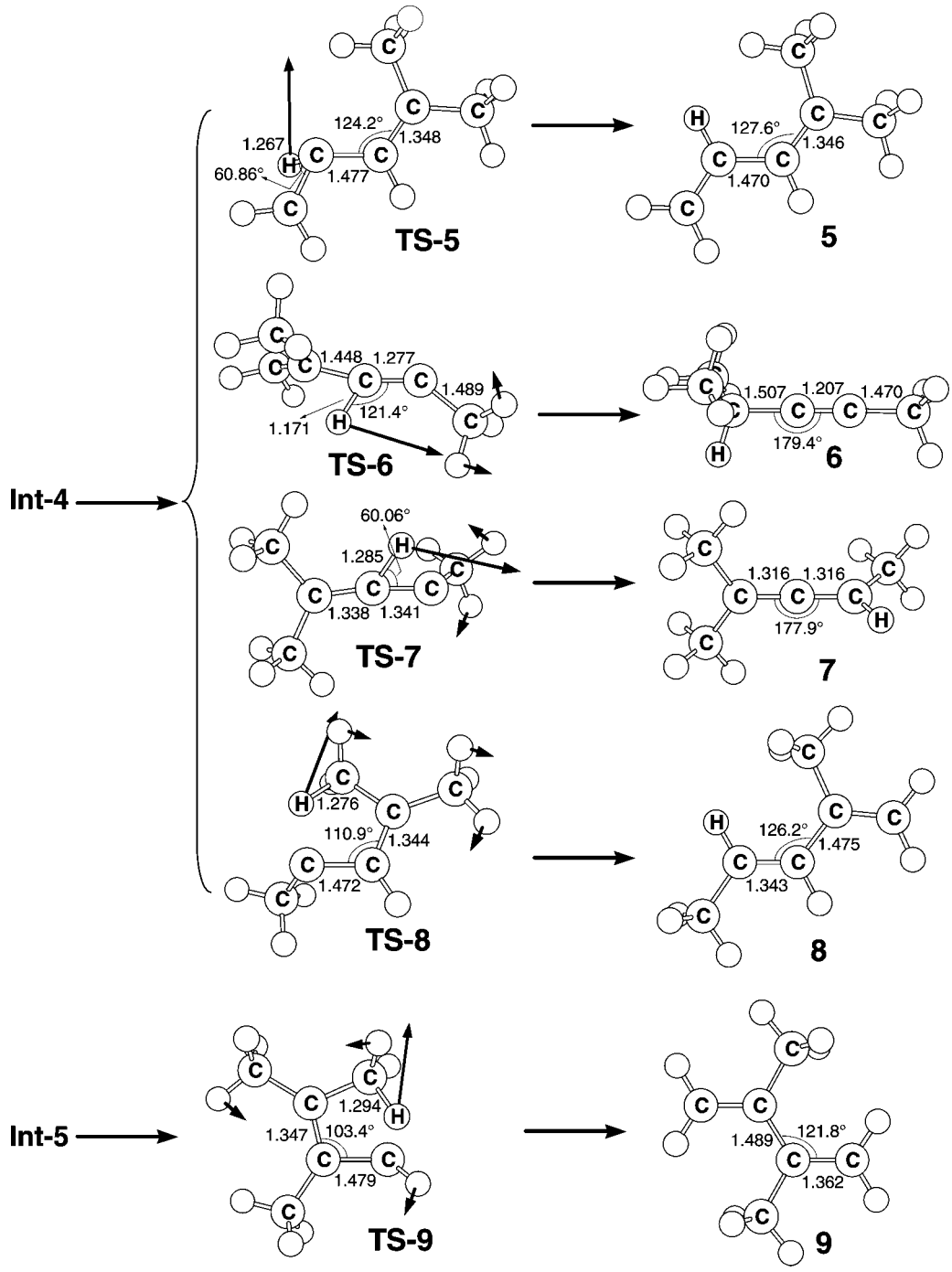

Figure 6. The CAS(6,6)/6−311G(d) geometries (in Å and deg) for path 7 of 1,3,3-trimethylcyclopropene (**4**), conical intersection (**CI**), and isomer product. The derivative coupling and gradient difference vectors—those which lift the degeneracy—computed with CASSCF at the conical intersections **CI-4**. The corresponding CASSCF vectors are shown inset. For more information see the Supporting Information.

FC-2 point but higher than the local intermediate **Int-3** by 10 kcal/mol. Accordingly, owing to the large excess energy (65 kcal/mol) obtained from the decay of **FC-2** to **Int-3**, it is expected that this relaxation energy is sufficient to drive the effective photoisomerization reactions (paths 5 and 6) for **4** (vide infra).

Furthermore, through the transition state **TS-4** (and **TS-4′**), the lowest energy point of the intersection seam of the S_0 and S_1 state was located for the ring opening process. This was identified as **CI-2** as presented in Figures 4 and 5. As suggested earlier, this can be equated to the more substituted vinylcarbene formed by cleavage of the C_1-C_2 cyclopropenyl bond. Then, funneling through the S_0/S_1 **CI-2** conical intersection can lead to two different reaction pathways on the ground-state surface via either the derivative coupling vector or the gradient difference vector.[10] The derivative coupling vector for **CI-2** corresponds to a C−C vibrating motion, which leads to a vibrationally hot species at the S_0 configuration. On the other hand, the gradient difference vector corresponds to a C−C bond stretching motion, which results in another planar intermediate **Int-4**. It should be noted here that although the energy is minimized,

Table 2. Energies (in kcal/mol) of the Critical Points Located along the Pathways 5-10 at the MP2-CAS(6,6)/6-311G(d,p)//CAS(6,6)/6-311G(d) and CAS(6,6)/6-311G(d) (in Parentheses) Levels of Theory[a]

structure	state	ΔErel[b]
1,3,3-trimethylcyclopropene **(4)**	S_0	0.0 (0.0)
FC-2	S_1	151.8 (172.9)
Int-3	S_1	87.51 (97.52)
TS-4	S_1	97.79 (107.1)
CI-2	S_1/S_0	46.67 (44.26)
Int-4	S_0	23.24 (26.19)
TS-5	S_0	35.75 (52.82)
5	S_0	−42.53 (−25.24)
TS-6	S_0	54.21 (65.82)
6	S_0	−32.82 (−31.00)
TS-7	S_0	39.63 (54.12)
7	S_0	−23.55 (−17.65)
TS-8	S_0	38.30 (62.64)
8	S_0	−34.96 (−31.43)
TS-4′	S_1	97.64 (106.3)
CI-3	S_1/S_0	61.93 (85.95)
Int-5	S_0	22.86 (50.74)
TS-9	S_0	61.14 (88.46)
9	S_0	−39.89 (−35.69)
TS-10	S_0	51.22 (49.47)
TS-11	S_0	62.41 (79.48)

[a] See Figures 5 and 6. [b] Energy relative to 1,3,3-trimethylcyclopropene (**4**).

the structure **CI-2** shown in Figures 4 and 5 is just a conical intersection rather than a true minimum,[10] because its energy gradient does not go to zero. Moreover the MP2-CAS computational results indicate that the energy of **CI-2** is 46 kcal/mol higher in energy than the ground-state minimum (**4**) and 105 kcal/mol lower than **FC-2**. The MP2-CAS results also demonstrate that the energy of **Int-4** is 129 kcal/mol lower than **FC-2** but 23 kcal/mol higher than that of the reactant **4**.

Again, after the local minimum **Int-4** on the S_0 potential energy surface is arrived at, there are four possible reaction pathways (**TS-5**, **TS-6**, **TS-7**, and **TS-8**) from which one may obtain the final photoproducts **5**, **6**, **7**,and **8**, respectively. Our MP2-CAS computations indicate that the barrier heights for these transition states from intermediate **Int-4** increase in the order **TS-5** (13 kcal/mol) < **TS-8** (15 kcal/mol) < **TS-7** (16 kcal/mol) < **TS-6** (31 kcal/mol). That is to say, our theoretical investigations are in reasonable agreement with the photoproduct distributions obtained experimentally.[6] Consequently, the calculations suggest that the reaction mechanisms for paths 5−8 should proceed as follows:

$$\text{Path 5: } \mathbf{4(S_0)} + h\nu \rightarrow \mathbf{FC-2} \rightarrow \mathbf{Int-3} \rightarrow \mathbf{TS-4} \rightarrow \mathbf{CI-2} \rightarrow \mathbf{Int-4} \rightarrow \mathbf{TS-5} \rightarrow \mathbf{5}$$

$$\text{Path 6: } \mathbf{4(S_0)} + h\nu \rightarrow \mathbf{FC-2} \rightarrow \mathbf{Int-3} \rightarrow \mathbf{TS-4} \rightarrow \mathbf{CI-2} \rightarrow \mathbf{Int-4} \rightarrow \mathbf{TS-6} \rightarrow \mathbf{6}$$

$$\text{Path 7: } \mathbf{4(S_0)} + h\nu \rightarrow \mathbf{FC-2} \rightarrow \mathbf{Int-3} \rightarrow \mathbf{TS-4} \rightarrow \mathbf{CI-2} \rightarrow \mathbf{Int-4} \rightarrow \mathbf{TS-7} \rightarrow \mathbf{7}$$

$$\text{Path 8: } \mathbf{4(S_0)} + h\nu \rightarrow \mathbf{FC-2} \rightarrow \mathbf{Int-3} \rightarrow \mathbf{TS-4} \rightarrow \mathbf{CI-2} \rightarrow \mathbf{Int-4} \rightarrow \mathbf{TS-8} \rightarrow \mathbf{8}$$

We have also explored the mechanism of path 9, which contains another conical intersection point (S_1/S_0 **CI-3**). As before, the structure of **CI-3** can be equated to the vinylcarbene derived from the cleavage of the less substituted cyclopropene σ-bond. The derivative coupling and gradient difference vectors obtained at the conical intersection are given in Figure 5. Our MP2-CAS results suggest that S_1/S_0 **CI-3** is lower in energy than **FC-2** by 129 kcal/mol but higher than the corresponding reactant **4** by 23 kcal/mol. The existence of a low-lying conical intersection provides a highly effective radiationless decay channel.[10] Besides this, the computations predict that the photochemical rearrangement reaction of path 9 should be the highest barrier process. That is, starting from the **FC-2** point, 1,3,3-trimethylcyclopropene (**4**) enters an extremely efficient decay channel, S_1/S_0 **CI-3**. After decay at this conical intersection point, this molecule will proceed via **Int-5** and **TS-9** points to reach the photoisomer **9**. Accordingly, this work suggests that the reaction mechanism for path 9 should be as follows:

$$\text{Path 9: } \mathbf{4(S_0)} + h\nu \rightarrow \mathbf{FC-2} \rightarrow \mathbf{Int-3} \rightarrow \mathbf{TS-4'} \rightarrow \mathbf{CI-2} \rightarrow \mathbf{Int-5} \rightarrow \mathbf{TS-9} \rightarrow \mathbf{9}$$

In addition, as shown in Figure 4, our computational results indicate that the two conical intersection points (i.e., **CI-2** and **CI-3**) are 47 and 62 kcal/mol lower in energy than **FC-2**, respectively. Competition between these reaction paths is presumably governed by the relative energies of the conical intersections involved. In consequence, the reaction paths through the **CI-2** point should be much more favorable through the **CI-3** point. Beside this, as discussed above, the reaction route through the **CI-2** point can lead to products **5**-**8** (path 5−8), while the reaction path through the **CI-3** point can only result in product **9** (path 9). Although these five routes (from path 5 to path 9) are competing with each other, only the last one is energetically unfeasible from a kinetic viewpoint. We would therefore expect a smaller quantum yield of **9** than of **5**-**8**. The energetic arguments are in qualitative agreement with the experimentally observed relative product distributions of **5**, **6**, **7**, **8**, and **9**, as already shown in eq 2.[6]

Before proceeding further, it should be pointed out that the first conical intersection (**CI-2**) is related to the more substituted vinylcarbene formed by cleavage of the cyclic (C_1-C_2) cyclopropenyl bond and producing the photoproducts **5**-**8**. Similarly, **CI-3** can be rationalized as arising from the less substituted vinylcarbene formed by cleavage of the cyclic C_1-C_3 bond and yielding photoproduct **9**. That is, the product distribution from photolysis is normally characteristic of reactivity associated with vinylcarbene intermediates, formed by cleavage of the C_1-C_3 or C_2-C_3 cyclopropene bonds in the first excited singlet state. As a result, our theoretical findings are in accordance with the predictions based on Fahie and Leigh's proposal.[6]

As in the case of cyclopropene (**1**), we also investigated the ground-state (thermal) potential surfaces of **4**, which are given in Figures 4 and 7. The search for transition states on the S_0 surface near the structures of S_1/S_0 **CI-2** gives **TS-10** and **TS-11**, which connect **4** and **8** and **4** and **9**, respectively. Our model calculations demonstrate that these transition states all involve a hydrogen migration with the calculated imaginary frequencies 148*i* and 152*i* cm^{-1}, respectively. In

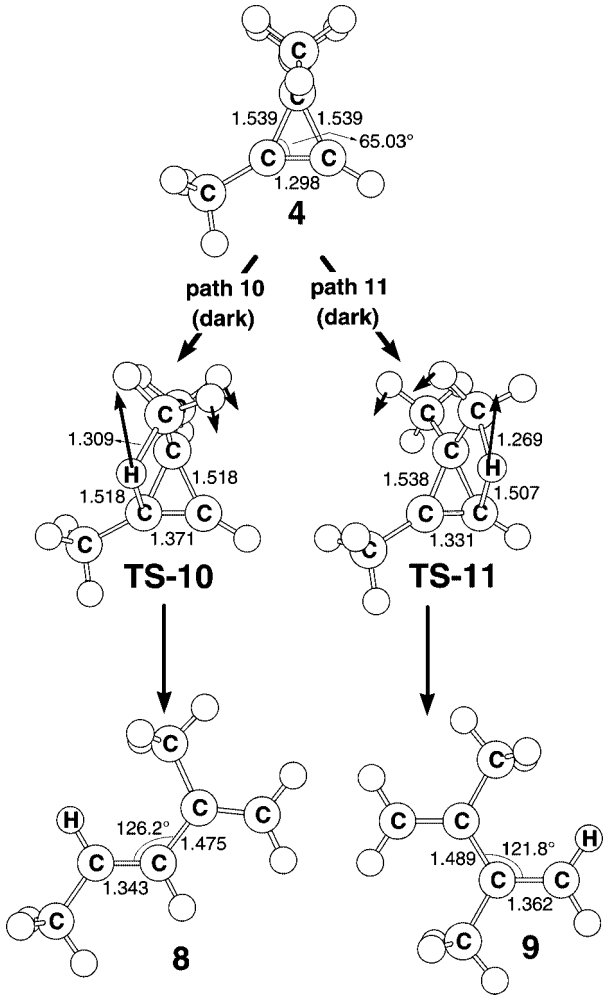

Figure 7. The CAS(6,6)/6−311G(d) geometries (in Å and deg) for path 8, path 9, and path 10 of spiro[2,4]hept-1-ene (**4**), transition state (**TS**), and isomer products in the dark (thermal) reactions. The heavy arrows indicate the main atomic motions in the transition state eigenvector. For more information see the Supporting Information.

consequence, our theoretical investigations suggest that the reaction mechanisms for paths 10 and 11 should proceed as follows:

$$\text{Path 10: } \mathbf{4} \rightarrow \mathbf{TS-10} \rightarrow \mathbf{8}$$

$$\text{Path 11: } \mathbf{4} \rightarrow \mathbf{TS-11} \rightarrow \mathbf{9}$$

Additionally, our theoretical work indicates that the barrier heights for these two reaction pathways are 51 and 80 kcal/mol, respectively. This strongly implies that path 10 should be the preferred route for the thermal reactions of **4**. Thus product **8** should have the largest yield. Again, our theoretical findings are in good agreement with the available experimental work.[7]

V. Conclusion

Photochemical mechanisms of cyclopropene **1** (eq 1) and 1,3,3-trimethylcyclopropene **4** (eq 2) have been investigated in the present work. Taking both systems studied in this paper together, one can draw the following conclusions:

(1) We summarize the results of the experimental and theoretical investigations of the photochemistry of cyclopropenes disscussed in this work in Scheme 4. In this scheme, we show the role of vinylcarbene intermediates in the photochemical and thermal reactions of cyclopropene and its derivatives. That is, our computational results are consistent with the intermediacy of a vinylidene species formed by ring opening. According to our theoretical findings, the vinylcarbene is formed in the S_1 (σp) state from the first excited singlet state of cyclopropene. It can then decay to photoproducts on the S_0 surface by 1,2-H migration. Our theoretical observations for the cyclopropene hydrocarbons are in good accordance with Leigh's experimental findings.[3]

Scheme 4

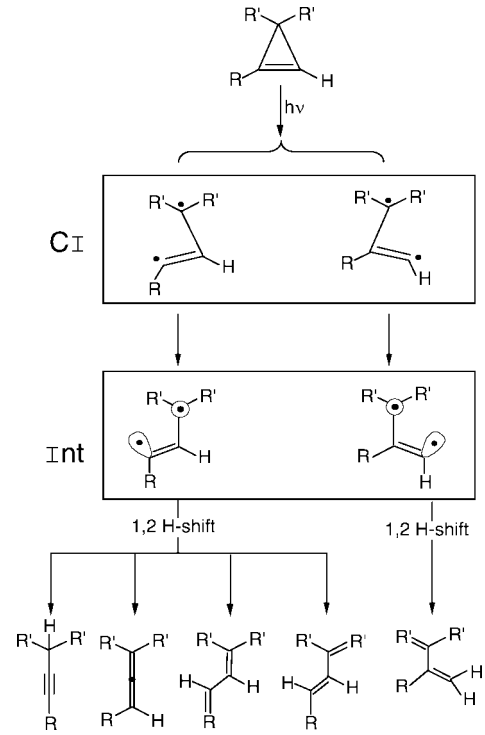

(2) Both cyclopropene and its derivative have a similar photochemical as well as thermal potential energy profile. Moreover, our calculations indicate that the differences between their energy barriers are not so large that small steric effects on the transition states would control the reaction mechanism as in other analogous molecular systems.

(3) From the present results, we can elaborate on the standard model of the photochemistry of cyclopropene and of its derivatives. It is found that knowledge of the conical intersection of the cyclopropene species is of great importance in understanding its reaction mechanism since it can affect the driving force for photochemistry. That is to say, the conical intersections can efficiently funnel molecules from the $^1(\pi\pi^*)$-state to the ground-state surface. Also, these funnels, which are easily accessed once the $^1(\pi\pi^*)$ surface is populated, determine the reaction path taken on the ground-state surface.[10] Accordingly, these findings, based on the conical intersection viewpoint, have helped us to better understand the photochemical reactions and to support the experimental observations.[3,6,7]

The photochemistry of cyclopropenes is seen to be intriguing in the varied types of photochemical reaction

encountered. In particular, the subtle variation provides both a mechanistic challenge and a promise of reward. It is hoped that the present work can stimulate further research into this subject.

Acknowledgment. The author is grateful to the National Center for High-Performance Computing of Taiwan for generous amounts of computing time and the National Science Council of Taiwan for the financial support. The author also wishes to thank Professor Michael A. Robb, Dr. Michael J. Bearpark (University of London, U.K.), and Professor Massimo Olivucci (Universita degli Studi di Siena, Italy) for their encouragement and support. Special thanks are also due to Reviewer 1 and Reviewer 2 for very helpful suggestions and comments.

Supporting Information Available: Details for the optimized atomic coordinates and energies of compounds studied in this work (PDF format). This material is available free of charge via the Internet at http://pubs.acs.org.

References

(1) For instance, see: (a) Greenberg, A.; Liebman, J. F. *Strained Organic Molecules*; Academic Press: New York, 1978. (b) Kobrich, G. *Angew. Chem., Int. Ed. Engl.* **1973**, *12*, 464. (c) De. Mayo, P. In *Rearrangements in Ground and Excited States*; Academic Press: New York, 1980, Vol. 3, p 501.

(2) For instance, see: (a) Padwa, A. *Org. Photochem.* **1979**, *4*, 261. (b) Padwa, A. *Acc. Chem. Res.* **1979**, *12*, 310. (c) Steinmetz, M. G.; Srinivasan, R.; Leigh, W. J. *Rev. Chem. Intermed.* **1984**, *5*, 57, and references cited therein.

(3) Leigh, W. J. *Chem. Rev.* **1993**, *93*, 487, and references cited therein.

(4) Chapman, O. L. *Pure Appl. Chem.* **1974**, *6*, 511.

(5) (a) Lifshitz, M.; Frenklach, M. J. *Phys. Chem.* **1975**, *79*, 1148. (b) Walsh, R. J. *Chem. Soc., Faraday Trans.* **1 1976**, *72*, 2137. (c) Bailey, I. M.; Walsh, R. J. *Chem. Soc., Faraday Trans.* **1 1978**, *74*, 1146.

(6) Fahie, B. J.; Leigh, W. J. *Can. J. Chem.* **1989**, *67*, 1859, and references cited therein.

(7) Srinivasan, R. J. *Chem. Soc., Chem. Commun.* **1971**, 1041.

(8) We will use the conical intersections to rationalize the mechanisms of the photoreactions of cyclopropenes. For details about conical intersections, see: Steinmetz, M. G.; Yen, Y.-P.; Poch, G. K. *J. Chem. Soc., Chem. Commun.* **1983**, 1504. (b) Reference 10. (c) Reference 11.

(9) It has been found that, according to many investigations of the reaction path of different organic reactions, in general, these processes are nonadiabatic; i.e., the path begins on an electronic excited state of the reactant species and ends on the ground-state energy surface where the product is formed. The central feature of such processes is that at some point along the excited-state reaction coordinate the system enters an efficiently decay channel, which takes the form of a conical intersection between the ground- and excited-state potential energy surfaces. Also see ref. (10).

(10) (a) Bernardi, F.; Olivucci, M.; Robb, M. A. *Isr. J. Chem.* **1993**, 265. (b) Klessinger, M. *Angew. Chem., Int. Ed. Engl.* **1995**, *34*, 549. (c) Bernardi, F.; Olivucci, M.; Robb, M. A. *Chem. Soc. Rev.* **1996**, 321. (d) Bernardi, F.; Olivucci, M.; Robb, M. A. J. *Photochem. Photobiol. A: Chem.* **1997**, *105*, 365. (e) Klessinger, M. *Pure Appl. Chem.* **1997**, *69*, 773. (f) Klessinger, M.; MichlJ. In *Excited States and Photochemistry of Organic Molecules*;VCH Publishers: New York, 1995.

(11) (a) Olivucci, M.; Ragazos, I. N.; Bernardi, F.; Robb, M. A. *J. Am. Chem. Soc.* **1993**, *115*, 3710. (b) Bernardi, F.; Olivucci, M.; Ragazos, I. N.; Robb, M. A. *J. Am. Chem. Soc.* **1992**, *114*, 8211.

(12) Frisch, M. J.; Trucks, G. W.; Schlegel, H. B.; Scuseria, G. E.; Robb, M. A.; Cheeseman, J. R.; Zakrzewski, V. G.; Montgomery, J. A., Jr.; Stratmann, R. E.; Burant, J. C.; Dapprich, S.; Millam, J. M.; Daniels, A. D.; Kudin, K. N.; Strain, M. C.; Farkas, O.; Tomasi, J.; Barone, V.; Cossi, M.; Cammi, R.; Mennucci, B.; Pomelli, C.; Adamo, C.; Clifford, S.; Ochterski, J.; Petersson, G. A.; Ayala, P. Y.; Cui, Q.; Morokuma, K.; Malick, D. K.; Rabuck, A. D.; Raghavachari, K.; Foresman, J. B.; Cioslowski, J.; Ortiz, J. V.; Baboul, A. G.; Stefanov, B. B.; Liu, Liashenko, G.; Piskorz, A.; Komaromi, P. I.; Gomperts, R.; Martin, R. L.; Fox, D. J.; Keith, T.; Al-Laham, M. A.; Peng, C. Y.; Nanayakkara, A.; Gonzalez, C.; Challacombe, M.; Gill, P. M. W.; Johnson, B.; Chen, W.; Wong, M. W.; Andres, J. L.; Gonzalez, C.; Head-Gordon, M.; Replogle, E. S.; Pople, J. A. Gaussian, Inc.: Pittsburgh, PA, 2003.

(13) Hehre, W. J.; Radom, L.; Schleyer, P. v. R.; Pople, J. A. *Ab Initio Molecular Orbital Theory*; Wiley: New York, 1986.

(14) Bearpark, M. J.; Robb, M. A.; Schlegel, H. B. *Chem. Phys. Lett.* **1994**, *223*, 269.

(15) (a) Gonzale, C.; Schlegel, H. B. J. *Chem. Phys.* **1989**, *90*, 2154. (b) Gonzale, C.; Schlegel, H. B. J. *Phys. Chem.* **1990**, *94*, 5523.

(16) McDouall, J. J. W.; Peasley, K.; Robb, M. A. *Chem. Phys. Lett.* **1988**, *148*, 183.

(17) (a) Steinmetz, M. G.; Srinivasan, R.; Leigh, W. J. *Rev. Chem. Intermed.* **1984**, *5*, 57, and references cited therein. (b) Padwa, A. *Acc. Chem. Res.* **1979**, *12*, 310. (c) Padwa, A. *Org. Photochem.* **1979**, *4*, 261.

(18) In addition to vinylcarbene formation from the first excited state, it was mentioned that other decay pathways (such as side-chain cleavage leading to free radicals) can intervene if the system bears appropriate substituents. See: (a) Reference 3. (b) Padwa, A.; Blacklock, T. J.; Cordova, D. M.; Loza, R. J. *Am. Chem. Soc.* **1980**, *102*, 5648.

(19) As pointed out by one referee, the geometry of intermediate **Int-1** is very interesting from the point of view of the chemical bond. In this three-membered ring species, two C—C bonds are tightly bonding (1.472 and 1.449 Å) and one C—C bond is nearly broken (1.827 Å). However, as discussed latter, this nearly broken C—C bond will be slightly closed together (about 1.714 or 1.771 Å) in the next excited transition state (**TS-1** or **TS-1′**) steps.

CT800078J